RESEARCH PAPER

PCCP
www.rsc.org/pccp

Free electron transfer mirrors rotational conformers of substituted aromatics: Reaction of benzyltrimethylsilanes with n-butyl chloride parent radical cations

Ortwin Brede,*[a] Ralf Hermann,[a] Sergej Naumov,[b] Antonios K. Zarkadis,[c] Gerasimos P. Perdikomatis[c] and Michael G. Siskos[c]

[a] *Interdisciplinary Group Time-Resolved Spectroscopy, University of Leipzig, Permoserstrasse 15, D-04303 Leipzig, Germany. E-mail: brede@mpgag.uni-leipzig.de*
[b] *Leibniz Institute of Surface Modification, Permoserstrasse 15, D-04303 Leipzig, Germany*
[c] *Department of Chemistry, University of Ioannina, 45110 Ioannina, Greece*

Received 11th February 2004, Accepted 2nd March 2004
First published as an Advance Article on the web 5th April 2004

The rotation motion of a larger substituent of an aromatic ring is accompanied by the electron density fluctuation of the highest occupied molecular orbitals. For benzyltrimethylsilanes *p*-R_3–C_6H_4–↻–$CR_1R_2(SiMe_3)$ [R_3 = H,PhCO; R_1, R_2 = H,H; H,Me; Me,Me; H,Ph; Ph,Ph] the silyl containing substituent rotates on the axis between the aromatic moiety and the benzylic carbon as indicated in the formula. In the course of this rotation a diversity of various conformers is passed. For the sake of simplicity, we reduce this diversity to two (extreme) borderline structures, one with the substituent in plane with the aromatic ring (transient), and one where the substituent is twisted by 90° (stable structure). In the very rapid and non-hindered electron transfer from the conformer mixture to n-butyl chloride parent radical cations, the singlet ground state conformers are converted into two kinds of radical cations. The cations tending to the planar type are stable whereas those of the twisted type dissociate immediately into benzyl type radicals (*p*-R_3–C_6H_4–$C^{\bullet}R_1R_2$) and trimethylsilyl cations. The above mentioned product pattern and quantum-chemical calculations on characteristic parameters of the ground state conformers and the product cations, show that the electron transfer occurs completely unhindered after diffusional encounter, *i.e.* after each approach of the reactants. Therefore the statistics of the rotation conformers mixture is reflected by the pattern and ratio of the product transients such as metastable radical cations and radicals derived from a dissociative radical cation. Up to now this is the only case where a diffusion-controlled electron transfer reaction proceeding in the nanosecond scale is influenced by intramolecular rotation motions within the electron donor.

Introduction

The photooxidation of alkyl and aryl substituted silanes has been the subject of various time-resolved and steady state experimental studies.[1,2] The co-sensitized oxidation of benzyltrimethylsilanes[3] is particularly interesting because the electron transfer process occurs decoupled of the primary excitation procedure. It can be analyzed as a proper ion–molecule reaction between the relaxed aromatic tetracyanobenzene radical cation ($C^{\bullet+}$) and the benzyltrimethylsilane, *cf.* reaction (1).

$$C^{\bullet+} + ArCH_2\text{–}SiR_3 \rightarrow C + ArCH_2\text{–}SiR_3\rceil^{\bullet+} \qquad (1)$$

It has been shown that in the non-polar surrounding the decay of the benzyltrimethylsilane radical cation proceeds in the nanosecond time scale. The C–Si bond cleavage occurs due to a S_N2 reaction with a nucleophile, or under distinct circumstances, in a monomolecular manner.[3,4]

$$ArCH_2\text{–}SiR_3\rceil^{\bullet+} (+Nu) \rightarrow Ar\text{–}CH_2^{\bullet} + R_3Si^{+} \qquad (2)$$

However, in the electron transfer from arylmethyl-trimethylsilanes to saturated parent radical cations derived from alkanes or alkyl chlorides, we found a primary simultaneous formation of two products such as the corresponding silane radical cations as well as benzyl type radicals,[5] both of them in similar amounts. The electron transfer from benzyltrimethylsilane to n-butyl chloride radical cations is represented by the following equation.

$$\text{n-}C_4H_9Cl^{\bullet+} + ArCH_2\text{–}SiMe_3 \rightarrow \text{n-}C_4H_9Cl + (Me_3Si^{+}) + ArCH_2\text{–}SiMe_3\rceil^{\bullet+} (\sim 40\%) + Ar\text{–}CH_2^{\bullet} (\sim 60\%) \qquad (3)$$

A few tenths of nanoseconds after the rapid and diffusion-controlled process (3), the part of silane radical cations was, in a delayed manner, converted to radicals according to reaction (2), which agrees well with the findings of Dockery *et al.*[3] Yet, the electron transfer mechanism (3) seemed to be quite different from the co-sensitized one given in reaction (1).

A behavior similar to reaction (3) has been recently observed during the electron transfer from phenols (ArOH), or other chalkogenols, to alkane and alkyl chloride radical cations ($RX^{\bullet+}$).[6–8] Comparable parts of phenol radical cations and phenoxyl radicals were formed simultaneously, and this unusual phenomenon could be explained using two basic arguments:

(i) the rotation of the phenol group around the C–O axis generates a mixture of extremely short-lived conformers with very different electron distributions of the highest molecular orbitals and

DOI: 10.1039/b402052a

(ii) a rapid non-adiabatic electron transfer takes place in each diffusive encounter between the reaction partners. That is why the rotation motion of the C–OH group is reflected by the formation of a stable phenol radical cation and a dissociative phenol radical cation, see reactions (4a,b), respectively. These products carry excess energy (*) which is lost in a few of picoseconds.

$$\begin{array}{l} RX^{\bullet+} + ArOH_{plane} \rightarrow \left[ArOH^{\bullet+*}\right] \rightarrow ArOH^{\bullet+} \\ \qquad\qquad \uparrow\downarrow \\ RX^{\bullet+} + ArOH_{perp} \rightarrow \left[Ar-O^{\bullet+}-H\right]^{*} \rightarrow ArO^{\bullet} + H^{+} \end{array} \qquad (4a, b)$$

The electron transfer in non-polar media involving parent solvent radical cations, derived from alkanes or alkyl chlorides, exhibits some peculiarities which are described in detail in refs. 9 and 11. Because of the high excess energy (0.5 to 2 eV) and the unusual uniform charge distribution over the whole sigma bonded skeleton of the parent cations,[9] this non-adiabatic electron transfer is very rapid. Therefore, it is called free electron transfer (FET) and is characterized by a non-hindered rapid electron jump.

Electron pulse radiolysis is the best method for the generation and kinetic study of the parent solvent radical cations. This method has also been used to investigate the kinetic problem illustrated in the aforementioned reactions (4a,b).

The aim of this paper is to analyze the unusual primary product behavior of the free electron transfer (FET) reaction (3) that involves bezyltrimethylsilanes with a varying substitution pattern at the benzylic carbon and in a *para*-position of the aromatic ring. In order to identify and quantify the product transients, pulse radiolysis experiments were conducted. Moreover, quantum chemical calculations were used to describe the dynamics of the substituent rotation.

Results and discussion

Experimental approach

Because of the high ionization potentials of the parent solvent molecules ($IP_{gas} \geq 10$ eV),[10] alkane and alkylchloride radical cations are very good electron acceptors. These cationic species represent complete σ-bond structured species where the charge is equally distributed over the whole skeleton. It results in their metastability ($\tau \leq 150$ ns) in liquid phase at room temperature.[11,12a]

Due to the unfavorable optical properties of alkenes and alkyl chlorides (light absorption in the far UV), electron pulse radiolysis has to be used for generating the parent ions and the study of the electron transfer involving appropriate donor molecules, see reactions (5) and (6). n-Butyl chloride is a useful solvent and acts as an internal electron scavenger. Hence the pulse radiolysis of n-butyl chloride generates mainly the following transients, *cf.* reaction (5):[13,14]

$$n\text{-}C_4H_9Cl \rightsquigarrow n\text{-}C_4H_9Cl^{\bullet+} + Cl^{-} + n\text{-}C_4H_9^{\bullet} \qquad (5)$$

$$n\text{-}C_4H_9Cl^{\bullet+} + D \rightarrow D^{\bullet+} + n\text{-}C_4H_9Cl,\ D = \text{electron donor} \qquad (6)$$

Under pulse radiolysis conditions in the nanosecond time scale reactions other than the diffusion-controlled electron transfer (6) can be excluded because of the much lower reactivity of the radiolytically formed radicals. Therefore we pulsed very diluted solutions of D ($c \approx 10^{-3}$ mol dm^{-3}) in n-butyl chloride where D stands for the different benzylsilanes used:

$$p\text{-}R^3\text{–}C_6H_4\text{–}CR^1R^2\text{–}SiMe_3$$

No.	R^1	R^2	R^3
1a	H	H	H
1b	Me	H	H
1c	Me	Me	H
1d	Ph	H	H
1e	Ph	Ph	H
2a	H	H	PhCO
2b	Me	H	PhCO
2c	Me	Me	PhCO
2d	Ph	H	PhCO
2e	Ph	Ph	PhCO

The time-resolved optical spectroscopy gave time profiles and optical transient spectra with an overall time resolution of the pulse radiolysis set up of < 10 ns, which is convenient for analyzing the bimolecular diffusion-controlled electron transfer reactions of type (6).

Kinetics of the free electron transfer (FET)

***p*-Benzoyl substituted benzylsilanes 2.** In the pulse radiolysis of pure n-butyl chloride, the optical transient absorption spectrum exhibits a broad absorption band between 350 and 650 nm ($\lambda_{max} = 500$ nm) of the parent ion n-$C_4H_9Cl^{\bullet+}$ with a life time $\tau = 140$ ns.[13,14] Adding to the sample millimolar concentrations of the silanes **1** and **2** shortens τ due to a pseudo-first order reaction. In the course of this reaction (6), product transient spectra appear (see Fig. 1) for the representative example of a 2×10^{-3} mol dm^{-3} solution of **2e**.

The spectrum of the nitrogen purged solution (Fig. 1a) taken after the 12 ns electron pulse in the maximum of the primary effect (80 ns), consists of three bands of a short-lived transient ($\tau = 2.1$ μs, $\lambda_{max} = 830$, 510 and 380 nm). They are superimposed on a long lasting absorption in the near UV ($\tau = 29$ μs, $\lambda_{max} = 350$ nm). The time profiles given on the top of Fig. 1 show the decay behavior of the two species which, in spite of the spectral superpositions, can be well distinguished. In the oxygen saturated solution, the short-lived transient is marginally influenced, whereas the long-lasting one seems to be converted into another long-lived species (see left part of Fig. 1b). In light of these observations and spectral analogies to literature data concerning the benzyltrimethylsilane radical cation,[15] the short-lived transient was assigned to the radical cation **2e**$^{\bullet+}$ whereas the more stable species was interpreted as a *p*-benzoyltriphenylmethyl radical[16,17] **2e**$^{\bullet}$ derived from **2e**$^{\bullet+}$ by dissociation (2).

The kinetics of the electron transfer (6) was analyzed in specified points of the spectrum, *i.e.* around the transient maxima. This is shown in Fig. 2 for the short time range, *i.e.* for the nanosecond scale. The decay of n-$C_4H_9Cl^{\bullet+}$ (620 nm) in tens of nanoseconds is described by $k_6 = 5.5 \times 10^9$ dm^3 mol^{-1} s^{-1}, and it corresponds well both with the formation of the silane radical cation **2e**$^{\bullet+}$ (840, 520 nm) and the rapid part of the fragment radical formation (350 nm). Judging the kinetics of the latter it should be taken into account that also the cation **2e**$^{\bullet+}$ decays by a delayed bond cleavage analogous to (2) and forming the triphenylmethyl type radical **2e**$^{\bullet}$. Hence there are two channels of radical formation, a rapid and direct one *via* electron transfer, and a delayed one *via* dissociation of the observed metastable cation **2e**$^{\bullet+}$, taking place with $k_8 = 4.8 \times 10^5$ s^{-1}. This mechanism is described by the reactions (7a,b) and (8). These reactions can be better distinguished by

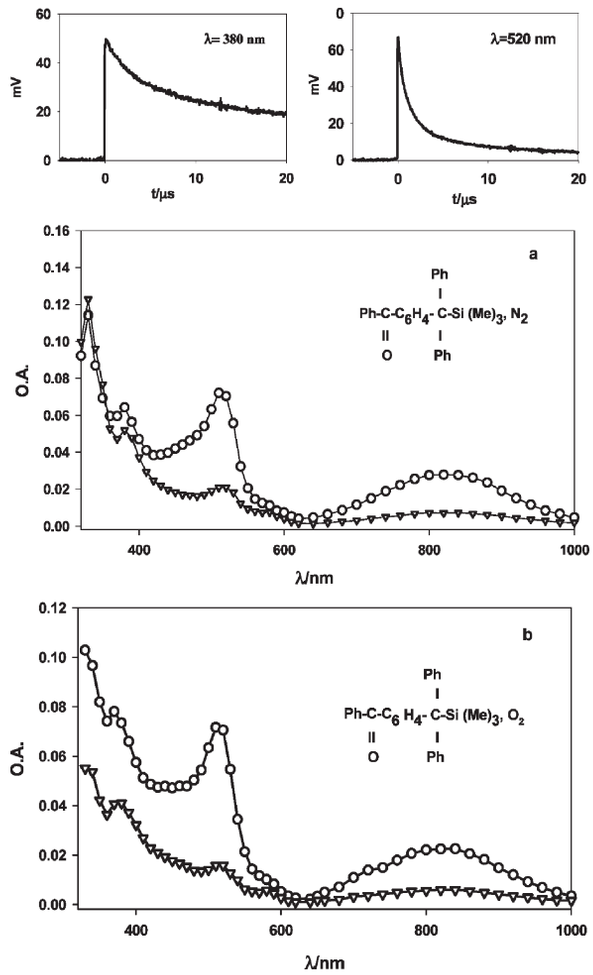

Fig. 1 Transient absorption spectra taken in the pulse radiolysis of a solution of 2×10^{-3} mol dm^{-3} **2e** in n-butyl chloride in the nitrogen purged sample (upper spectra, a) and in oxygen saturated solution (lower spectra, b), times after the pulse: (○) 80 ns, (▽) 18 μs (for a, N_2) or 3.5 μs (for b, O_2). The time profiles on the top of the figure were taken in N_2 bubbled solution: 380 nm mainly for a radical **2e**$^{\bullet}$, 520 nm representative for **2e**$^{\bullet+}$.

comparing the time profiles of the radical absorption at 350 nm in N_2 purged and in O_2 saturated solution, see Fig. 2. In the first case the rapid (7b) and the delayed (7a), (8) radical formations are well observable. In the second one, oxygen quenches mainly the delayed formation (8) and, therefore,

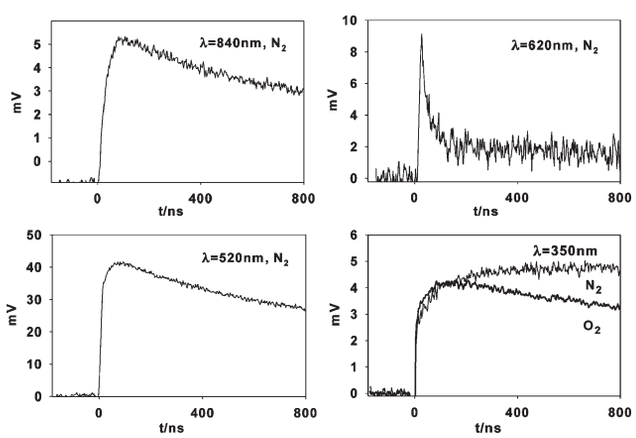

Fig. 2 Time profiles of the n-$C_4H_9Cl^{\bullet+}$ (620 nm), the silane radical cation **2e**$^{\bullet+}$ (840, 520 nm) and the fragment radical **2e**$^{\bullet}$ (350 nm) taken in the pulse radiolysis of a solution of 2×10^{-3} mol dm^{-3} **2e** in n-butyl chloride purged with nitrogen (at 350 nm also treated with O_2).

the electron transfer part (7b) is visualized. This complex kinetic situation is presented in the following reaction sequence (7)–(10).

$$PhCO\text{-}C_6H_4\text{-}CPh_2\text{-}SiMe_3 + n\text{-}C_4H_9Cl^{\bullet+} \quad (7)$$

$$\xrightarrow{k_{7a}} PhCO\text{-}C_6H_4\text{-}CPh_2\text{-}SiMe_3]^{\bullet+}$$

$$\xrightarrow{k_{7b}} n\text{-}C_4H_9Cl$$

$$PhCO\text{-}C_6H_4\text{-}CPh_2\text{-}SiMe_3]^{\bullet+} \xrightarrow{k_8} PhCO\text{-}C_6H_4\text{-}(Ph_2)C^{\bullet} + Me_3Si^{+} \quad (8)$$

$$+O_2 \xrightarrow{k_9} \text{products} \quad (9)$$

$$+O_2 \xrightarrow{k_{10}} PhCO\text{-}C_6H_4\text{-}(Ph_2)COO^{\bullet} \quad (10)$$

Both the silane radical cation **2e**$^{\bullet+}$ and the fragment radical are sensitive to oxygen with k_9 around 5×10^7 dm^3 mol^{-1} s^{-1} and k_{10} in the range of 10^9 dm^3 mol^{-1} s^{-1}, where the latter is difficult to calculate because of spectral superpositions with the produced peroxyl radical. A similar value of $k_{10} = 3 \times 10^8$ M^{-1} s^{-1}, typical for trityl radicals, has been reported for the reaction of the *p*-benzoyltriphenylmethyl radical with oxygen.[17]

A similar reaction behaviour was also found for the other benzoyl substituted silanes of type **2**. Fig. 3 demonstrates spectra and decay kinetics of the silane radical cations and fragment radicals derived from the methyl substituted compound **2b**. Here the silane radical cation **2b**$^{\bullet+}$ with bands at 640 and 400 nm as well as the radical signal at 340 nm can be easily distinguished. It can be seen that the rapidly formed radical part (analogous to reaction (7b)) is quenched by oxygen already in an early state. The remaining absorption around 340 nm is caused by the resulting peroxyl radical. The decay time profiles taken at 400 and 340 nm (Fig. 3) demonstrate the relatively clean decay of **2b**$^{\bullet+}$, whereas the radical time profile follows a more complex kinetics—rapid (7b) and delayed (8) formation of the radical, and slightly superimposed with the cation absorption tail. The kinetic data for **2b** and the other compounds of type **2** are summarized in Table 1.

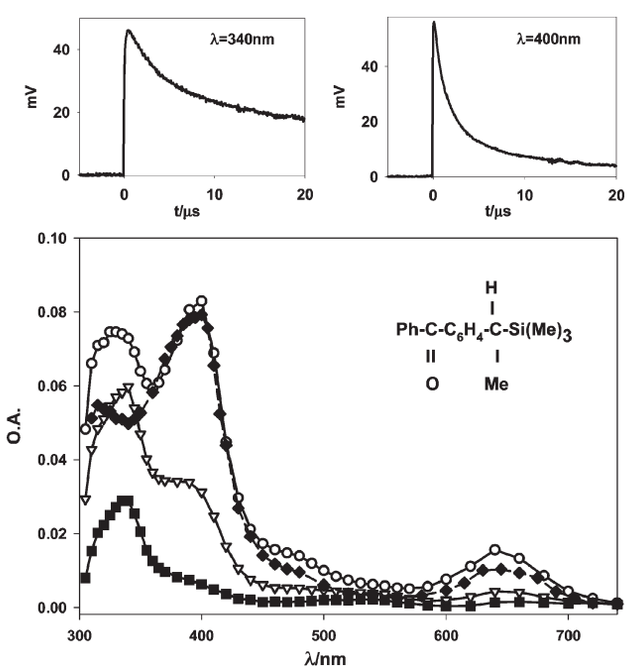

Fig. 3 Transient absorption spectra taken in the pulse radiolysis of a solution of 1.2×10^{-3} mol dm^{-3} **2b** in n-butyl chloride. N_2 purged solution: 100 ns (○), 3 μs (▽) and 18 μs (■) after the pulse; O_2 saturated solution: after 100 ns (◆). The time profiles demonstrate the typical transient decay behavior: 340 nm mainly **2b**$^{\bullet}$, 400 nm for **2b**$^{\bullet+}$.

Table 1 Kinetic and spectral parameters of the product formation by free electron transfer from benzyltrimethylsilanes to n-butyl chloride radical cations

	$k_{7a,b}$ of FET/ dm^3 mol^{-1} s^{-1}	Silane radical cations		Benzyl type radicals		k_{10}, O_2 rct./dm^3 mol^{-1} s^{-1}	Product ratio cat./rad.
		λ_{max}/ nm	τ_{decay}/ ns	λ_{max}/ nm	τ_{decay}/ μs		
1a	5×10^9	530 310	290	320, *260*	12	10^9	40/60
1b	5×10^9	550 315	140	320, *260*	>30	10^9	30/70
1c	diff.-contr.	450 330	<100	320, *270*	30		
1d	4×10^9	450 330	100	330	40	7×10^8	30/70
1e	diff.-contr.	480–520	<70	340	40	7×10^8	25/75
2a	5×10^9	620 380	1500	330	20	5×10^8	40/60
2b		640 400	2800	340	20		
2c		670 410	1400	340	28		
2d		760 525 380	2800	345	38	10^9	
2e	6×10^9	830 510 380	2100[a]	350	29	10^9	25/75

[a] k_9 with oxygen $= 5 \times 10^7$ dm^3 mol^{-1} s^{-1}.

FET producing less stable benzyltrimethylsilane radical cations. The benzyltrimethylsilanes of type **1** were found to generate less stable radical cations than the *p*-benzoyl substituted ones of type **2**. Therefore their reaction is discussed after the principal studies given in the preceding paragraph. Fig. 4 presents transient absorption spectra obtained in the pulse radiolysis of a 1.8×10^{-3} mol dm^{-3} solution of the silane **1a** in n-butyl chloride.

Partially in accordance with the literature[3] and also because of the kinetic behavior, the two absorption maxima of the short-lived transient ($\tau = 290$ ns, $\lambda_{max} = 530$ and 310 nm) were assigned to the metastable silane radical cation **1a**$^{\bullet+}$. The longer-lasting absorption bands ($\tau = 12$ μs, $\lambda_{max} = 320$ and 260 nm) are interpreted to be caused by the benzyl radical **1a**$^{\bullet}$, which is well known from the literature.[18] As already mentioned, in the presence of oxygen a marked part of the benzyl absorption ≤320 nm is quenched from the very beginning. It gives arguments for its rapid and direct formation by the electron transfer, analogous to the reaction path (7b). The time profiles shown in Fig. 5 illustrate the FET kinetics in more detail. At 640 nm only the decay of n-$C_4H_9Cl^{\bullet+}$ is observed, at 530 nm a superposition of the n-$C_4H_9Cl^{\bullet+}$ and the silane cation **1a**$^{\bullet+}$ appears, and at 310 nm the kinetics of **1a**$^{\bullet+}$ could be seen clearly. The radical signal at 260 nm shows the rapid radical formation by (7b) and the delayed one *via* the cation **1a**$^{\bullet+}$ by reactions (7a) and (8). All silane species were found to be formed with a rate constant $k_{7a,b} = 5 \times 10^9$ dm^3 mol^{-1} s^{-1}, *i.e.* with a diffusion-controlled rate.

Analyzing the quenching of the transients by oxygen it should be mentioned that because of its short lifetime the radical cation **1a**$^{\bullet+}$ does not show any effect. The benzyl radical is quenched with k_{10} of about 10^9 dm^3 mol^{-1} s^{-1} where, because of spectral superpositions, the exact value is difficult to determine.

The other silanes of type **1** show an analogous kinetic behavior. In the case of higher substitution at the benzylic carbon atom it was observed that the lifetime of the silane radical cations becomes shorter. For the triphenyl substitution pattern **1e**, in the red range a signal peaking different from that of n-$C_4H_9Cl^{\bullet+}$ was found and it is assigned to **1e**$^{\bullet+}$. However, because of a lifetime ≤50 ns, it could not be kinetically distinguished from the solvent parent ion. The spectral and kinetic data of the transients produced by FET ionization of the benzyltrimethylsilanes **1** and **2** are summarized in Table 1.

Interpretation of the FET kinetics and its product distribution. In the free electron transfer from the benzyltrimethylsilanes to the solvent parent ions n-$C_4H_9Cl^{\bullet+}$ two kinds of products are directly observed and formed with the same rate, namely the benzyltrimethylsilane radical cations and the benzyl type radicals. Subsequently, the metastable silane radical cations are transformed into benzyl type radicals in a delayed process. The transformation can be well seen in the radical time profile (*cf.* Fig. 2, 350 nm profile; Fig. 5, 260 nm profile). In the cases when the spectral transient superposition is not too strong, the ratio between the two reaction channels (7a) and (7b) can be estimated from the fast and delayed parts in the radical time profile. In the case of **1a**, about 40%silane radical cations (path (7a)) and 60% radicals (path (7b)) were formed by FET. The product distribution of the FET varies predominantly between 20 and 40% silane radical cations and hence the benzyl type radicals dominate with 80 to 60% (see Table 2). Because of

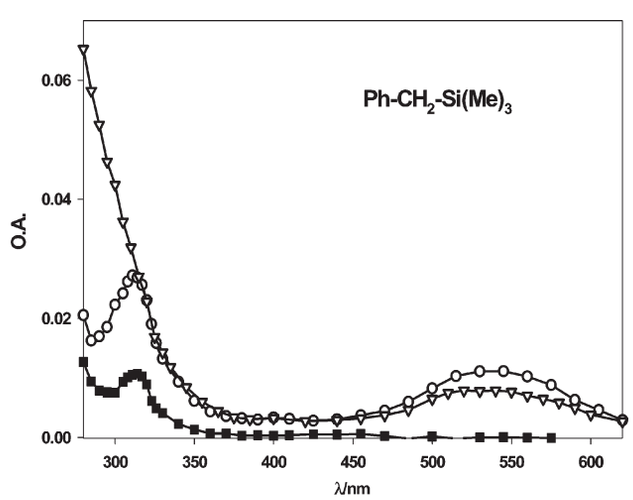

Fig. 4 Transient absorption spectra taken in the pulse radiolysis of a solution of 1.1×10^{-3} mol dm^{-3} **1a** in n-butyl chloride. N_2 purged solution: 100 ns (○) and 2 μs (■) after the pulse; O_2 saturated solution: after 100 ns (▽).

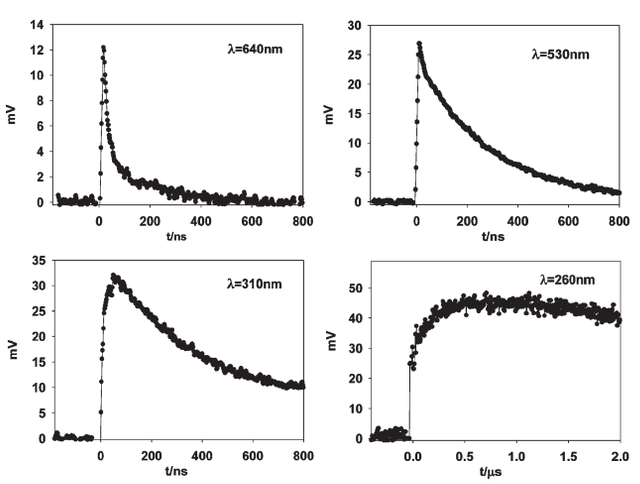

Fig. 5 Time profiles of the n-$C_4H_9Cl^{\bullet+}$ (640 nm), the silane radical cation **1a**$^{\bullet+}$ (530, 310 nm) and the benzyl radical **1a**$^{\bullet}$ (partially at 310 nm, main part 260 nm) taken in the pulse radiolysis of a solution of 2×10^{-3} mol dm^{-3} **1a** in n-butyl chloride purged with nitrogen.

Table 2 Calculated (B3LYP/6-31G(d)) parameters[a]

	R^1	R^2	R^3	Structure	τ_{Rot}/ps	E_a/kcal mol^{-1}	C–Si/Å Singlet	C–Si/Å Radical cation	Δ(C–Si)/Å	S(Si)
1a	H	H	H	Stable	1.33(0.43)[b]	3.8(15.7)[b]	1.919	2.082	0.163	0.096
				Tr. St.			1.910	1.942	0.032	~0.00
1b	H	Me	H	Stable	0.9	5.7(19.4)[b]	1.929	2.138	0.209	0.114
				Tr. St.			1.934	1.963	0.029	~0.00
1c	Me	Me	H	Stable	1.8(0.46)[b]	3.9(20.8)[b]	1.946	2.211	0.265	0.134
				Tr. St.			1.946	1.974	0.028	~0.00
1d	H	Ph	H	Stable	0.9	2.3	1.939	2.164	0.225	0.118
				Tr. St.			1.948			
1e	Ph	Ph	H	Stable	2.0		1.997	2.365	0.368	0.149
2a	H	H	ArCO	Stable	1.45(0.84)[b]	4.4(11.5)[b]	1.922	2.025	0.103	0.064
				Tr. St.			1.913	1.935	0.022	~0.00
2b	H	Me	ArCO	Stable	2.04	5.6(13.5)[b]	1.933	2.080	0.147	0.085
				Tr. St.			1.930	1.960	0.030	0.005
2c	Me	Me	ArCO	Stable	2.19(1.59)[b]	3.5(13.9)[b]	1.950	2.140	0.190	0.104
				Tr. St.			1.948	1.967	0.019	~0.00
2d	H	Ph	ArCO	Stable	2.04	2.1	1.945	2.135	0.190	0.105
				Tr. St.			1.953			
2e	Ph	Ph	ArCO	Stable	2.38	2.5	1.996	2.308	0.312	0.135
				Tr. St.			1.999			

[a] τ_{rot} and activation energies (E_a) of the trimethylsilyl-group rotation, bond length C–Si for the ground state and the radical cation and bond length change Δ(C–Si) in dependence on molecular geometry. S(Si)—atomic spin density on Si atom of radical cation. Tr. St.—transition state structure. [b] Radical cation value in parentheses.

the aforementioned spectral superpositions these ratios represent very rough measures. No such estimates could be made in the cases where the UV main radical band (around 260 nm) is covered by the silane own absorption.

In order to understand the reason for this unusual reaction behaviour, a former result that takes into account the peculiarities of the free electron transfer has to be highlighted. As far as the parent radical cations are concerned, the even distribution of the charge over the whole σ-bond skeleton of alkanes[8,12b,c] and alkyl chlorides[8,12a] as well as the relatively large ionzation potential differences between donor and acceptor ($\Delta IP \geq 0.5$ eV) impose a non-hindered electron transfer step. The non-hindered electron transfer step occurs practically in each encounter between the reactants. Therefore the electron transfer works in each encounter geometry of the molecular electron clouds, *i.e.* also without a defined encounter state in the usual sense. Such a picture is typical for a non-adiabatic electron transfer which can happen also *via* longer distances. If each approach of the reactants succeeds in electron transfer, then the rotation motions within the electron donor molecule can play a role. This is true in particular for the rotation motions of substituents at aromatic rings. As already mentioned in the Introduction, when the FET involves phenols, the rotation of the –OH group around the C–O axis is reflected by two different kinds of products. These products originate from a metastable phenol radical cation and dissociative phenol radical cation, respectively, *cf.* reaction (4a,b).

To explain the molecule dynamic effect reported in this paper the following points are to be considered:

—The donor substances (benzyltrimethylsilane type compounds) exhibit a rotation motion around the bond between the aromatic ring and the substituent as indicated by the arrow *p*–R_3–C_6H_4—$CR_1R_2(SiMe_3)$ with a frequency around 10^{12} Hz. Statistically seen, during the rotation motion all imaginable twist angles between 90° (stable state) and 0° (transition state) are passed. The manifold of these twisted extremely short-living structures is difficult to describe by a simple picture. Therefore we used only the extreme cases (90°, 0°) and called them border line structures. It means that the diversity of all other twisted structures is contained either in the 90° conformer or in that of 0° angle and it is determined by the electron distribution in the ground state.

—The free electron transfer takes place during the first approach of the reactants (as a non-adiabatic and longer-range interaction). The electron transfer of two characteristic kinds of products indicates the diversity of the short-living conformers that are being continuously formed by the rotation motion.

Also in the case of the benzyltrimethylsilanes studied here, the rotation of the substituent around the axis connecting the aromatic moiety and the benzylic carbon (see also Scheme 1). is accompanied by electron fluctuation at the HOMO level. As a consequence, metastable silane radical cations (7a) with

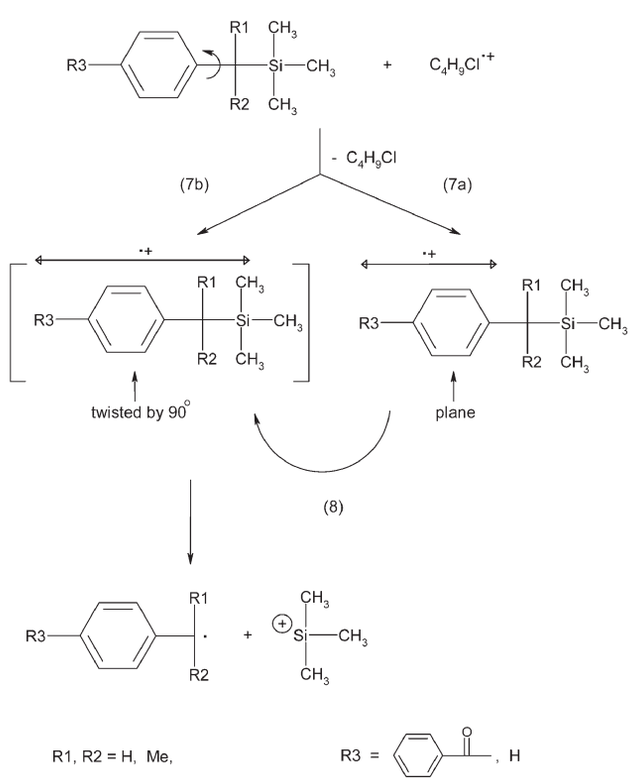

Scheme 1

charge at the aromatic ring as well as those with their charge partially localized also at the benzyl carbon (7b) are formed, where the latter dissociates immediately. On the other hand the partially hindered rotation of the benzylic bond seems to cause the delayed dissociation (8), see the preceeding chapter.

Quantum-chemical calculations

Quantum-chemical calculations with 10 molecules bearing different substituents in the positions R1, R2 and R3 were performed in order to support the proposed mechanism[5] of the generation of two different radical cations in dependence on the molecular structure. All of the studied molecules behave similarly. The equilibrium geometries of the singlet ground state and of the radical cation have a C–Si bond nearly perpendicular to the ring plane (dihedral angle C2–C1–C7–Si nearly 90°). The frequency analysis of the singlet ground state shows the existence of a relatively slow (from 0.4×10^{12} to 1.1×10^{12} Hz depending on the substituents) rotation motion around the axis connecting the benzylic and the *ipso*-aromatic carbon atom. This leads to a "planar structure" (C–Si bond coplanar to the ring plane). The frequency analysis of the "planar structures" produces only one imaginary frequency indicating that this conformation represents the transition state for rotation. The activation energies (barrier heights of rotation) E_a calculated for the molecules in the ground state are between 2.3 and 5.7 kcal mol^{-1} and, hence, at room temperature the internal rotation of the trimethylsilyl-group should proceed. However, if the radical cation is generated, the activation energy for rotation is found to be essentially higher, *i.e.*, the rotation motion should be strongly hindered.

This is also expected considering imaginary resonance forms and the extended stabilisation provided by the β-silicon effect,[19] see Scheme 2. The calculated data for the stable (perpendicular) and transition (planar) structures are given in Table 2.

The calculated valence C–Si vibrations have a frequency of about 2.7×10^{13} Hz corresponding with a time for one vibration of about 37 fs and being at least 30 times faster than the rotation of the $–CR^1R^2–SiMe_3$ group. Yet, both of them are slow in comparison to the electron transfer jump. According to the Born–Oppenheimer approximation and due to the relatively slow internal rotation of the substituent $–CR^1R^2–SiMe_3$, the molecular geometry is stiff relative to the electron relaxation process and the very fast electron transfer event. In order to test the influence of the molecular geometry on the electronic structure, we investigated the behaviour of the highest double occupied MO (HOMO) of the singlet ground state. This state is involved in the electron transfer process, in dependence on $–CR^1R^2–Si(Me)_3$ group rotation (torsion angle φ).

The changes of electron distribution from HOMO show a similar trend (as shown in case of **1a** in Fig. 6) in all the studied molecules. As can be seen from Fig. 6, the σ C–Si bond is formed through an sp^3 hybrid from carbon and Si atoms. In the stable perpendicular structure this σ-bond has the same

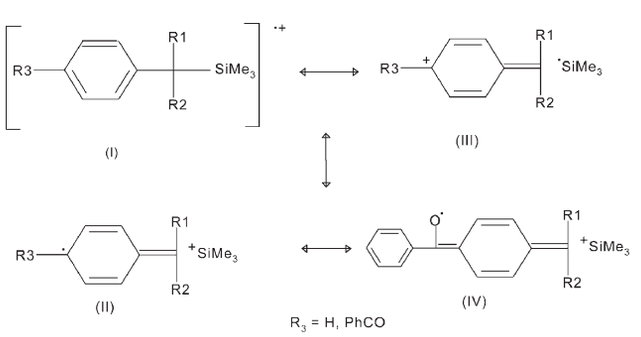

Scheme 2

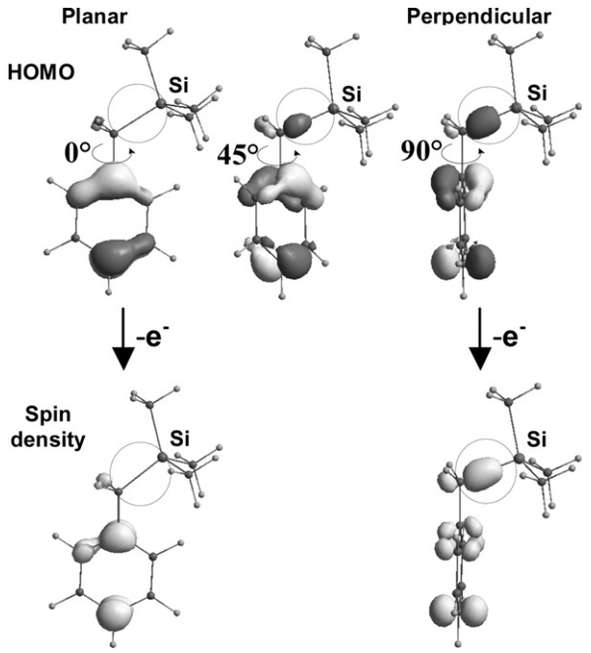

Fig. 6 Transformation of HOMO of the **1a** singlet ground state (isocontur = 0.08) in dependence on C–$Si(Me)_3$-group rotation and spin density distribution of the radical cation (isospin = 0.01).

symmetry as the π system of the aromatic ring. Due to the strong resonance with the π electron of the aromatic ring, the electron from HOMO is partly shifted from the aromatic moiety to the C–Si bond. By a rotation around the C–Si bond the coupling between ring and sp^3 hybrid from C–Si bond will be disturbed.

Therefore the HOMO in the planar structure is entirely localized on the aromatic ring. It should be mentioned that according to the Hammet rules the $–CH_2SiMe_3$ group is an electron donating substituent in electrophilic aromatic substitutions[20] with a σ_p constant of −0.21.

Thus, due to the relatively slow rotation motion, after electron transfer from the HOMO of $Ar–CH_2–Si(Me)_3$ to the solvent radical cation two different radical cation types can be generated. In the "perpendicular" radical cation the unpaired electron is partly localized on the C–Si bond. It leads to a strong weakening of this bond in the radical cation state. In the planar radical cation, there is no unpaired electron on the C–Si bond and, consequently, the bond length should not be influenced coming from the ground to the radical cation state.

With respect to these results and for a sufficiently short time scale where the rotation of the critical bond is "frozen," we can assume two limiting conformer structures strongly differing in the tendency to a prompt dissociation, in correspondence with eqns. (7a,b).

This different behaviour of the HOMO electrons is strongly supported by calculations of C–Si bond length changes (Δ(C–Si)) between the ground and the radical cation state, in dependence on molecular geometry. While in the planar structure the C–Si bond is practically unchanged, in the case of the perpendicular structure it becomes longer (up to 0.368 Å for **1e**), see Table 2. Thus, the radical cations in the perpendicular structure seem to be less stable than those in the planar one and, therefore, they are favoured for a rapid desilylation. Additionally, there is a strong dependence of the Δ(C–Si) on the type of the substituents R1, R2 and R3 (Table 2), which correlates clearly with the atomic spin density on Si calculated for the perpendicular radical cation (see Fig. 7a). The more the unpaired electron resides on Si, the larger is the change of Δ(C–Si) and, consequently, the weaker is the C–Si bond and the shorter is the life time of the radical cations.

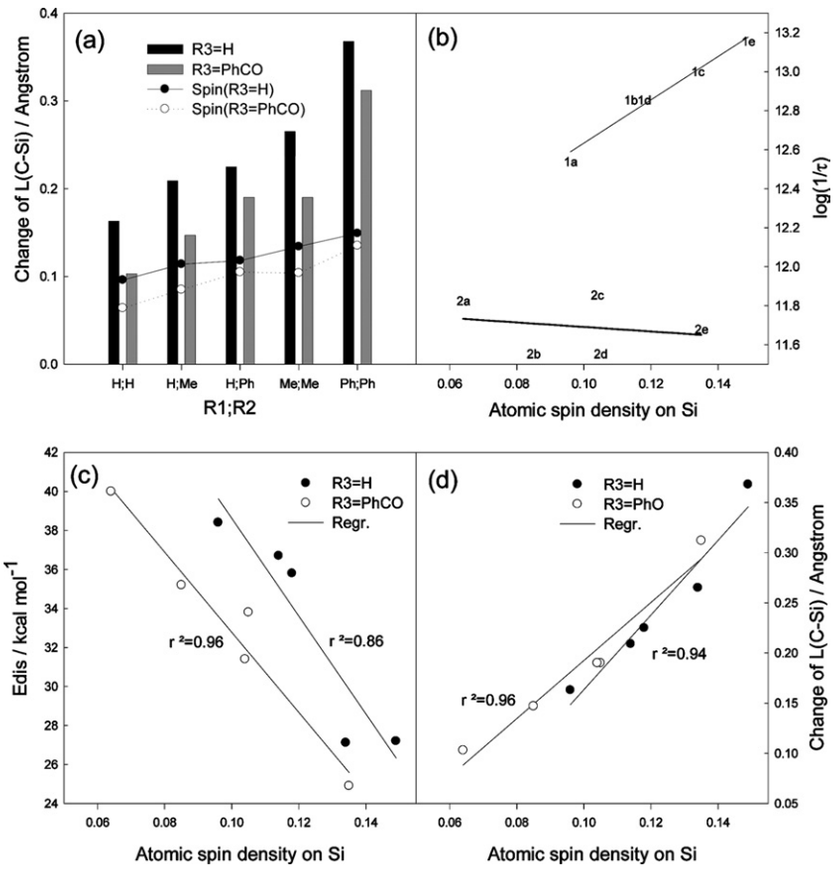

Fig. 7 (a) Calculated for radical cations: spin densities on Si-atom and C–Si bond length changes (Δ(S–Si)) between ground state and radical cation state in dependence on substituent R1, R2 and R3. (b) Correlations between calculated spin densities on Si-atom and the experimental decay rate constant ($1/\log \tau_{decay}$, originating from Table 1) of radical cations in dependence on substituent R1, R2 and R3. Correlations between the spin densities on the Si-atom and (c) the bond dissociation energy of the C–Si bond of the radical cations $\mathbf{1}^{\bullet+}$ and $\mathbf{2}^{\bullet+}$, or (d) change of the C–Si bond in these radical cations.

The compatibility of the data can be also seen from the correlations given in Fig. 7a–d where the spin densities of the different cations $\mathbf{1}^{\bullet+}$ and $\mathbf{2}^{\bullet+}$ are plotted against the lifetime, cation dissociation energies and bond lengths changes of the C–Si bond.

Preliminary concluding the results of the quantum-chemical analysis, the two types of benzyltrimethylsilane radical cations should be qualified as

—*stable* ones (non-dissociative) with planar structure and charge positioned at the aromatic ring, decaying by statistical transformation into the perpendicular state, and

—*dissociative* ones with perpendicular structure and charge distribution over the whole molecule, decaying during the C–Si bond vibration.

As far as perpendicular radical cation is concerned, the above conclusions are in line with the often used tentative and qualitative resonance structures given by the formulae (I) to (IV). It is obvious that the structure (IV) of the *p*-benzoyl derivatives is responsible for the diminished spin density found on Si (Fig. 7). The importance of (IV) is also demonstrated in EPR spectra of the *p*-benzoyltriphenylmethyl radical[21] where the *p*-benzoyl group causes an approximately 18% shift of the spin density to the *p*-benzoyl substituted ring. On the other hand within each series (R_3 = H or PhCO), an increasing substitution on the benzylic carbon causes an increase in the spin density at Si due to increased contribution of (III). Therefore it is resonable to assume that (III) contributes more to R3 = H than to R3 = PhCO. It explains (i) the larger bond length changes Δ(C–Si), (ii) the lower activation energies of the Ar–CSi bond rotation and (iii) the corresponding higher decay rate constants (Tables 1, 2 and Fig. 7b) for R_3 = H than for R_3 = PhCO. The diminished importance of (III) for R_3 = PhCO is also indicated by the observation that benzylic substitution within this series does not affect E_a or $\log(1/\tau)$ significantly.

Electron transfer involving σ- or π-type radical cations

Comparing the results of the (cosensitized) electron transfer[3] (reaction (1)) with those of the FET described in this paper, the reason for the different product distribution comes into question. In the case of cosensitization when a π system stabilized acceptor radical cation was used, exclusively benzylsilane radical cations were formed, *cf.* reaction (1). The process follows the usually assumed reaction path proceeding through the formation of an encounter complex. This results from encounter of an aromatic π-stabilized radical cation with the donor molecule. The encounter leads to the formation of an energetically favored complex which is optimized in the course of the donor–acceptor interaction. Next a controlled electron transfer (1) occurs. The transfer can be imagined as a concerted electron transition with bond length change in the participating molecules, which results in one dominating product, here the donor radical cation only. A situation has been reported for the case of the electron transfer from phenols to benzene radical cations. There a controlled sandwich-like encounter complex has been described by a quantum chemical approach.[22]

$$C_6H_6^{\bullet+} + \text{Ar–OH} \Leftrightarrow [C_6H_6^{\bullet+} \cdots \text{Ar–OH}] \Leftrightarrow [C_6H_6 \cdots \text{Ar–OH}^{\bullet+}] \Leftrightarrow C_6H_6 + \text{ArOH}^{\bullet+} \quad (13)$$

On the other hand, σ-type parent radical cations derived from alkanes or alkyl chlorides are metastable species

stabilized only by the equilibration of the charge over the whole molecule. In the light of the above mentioned results and taking into account the very high free energy of (up to 2 eV) of the free electron transfer in non-polar systems, it can be said that every single approach regardless of its geometry succeeds in an electron transfer, apart from an optimized encounter complex. Therefore only the direct forward reaction path of reaction (6) is to be considered. If the donor molecule contains a defined rotating group, then this motion is accompanied by electron fluctuations of the highly occupied orbitals along the molecule. Consequently, the molecule conformation is permanently changed with a relatively high frequency and on the average it results in a mixture of the diverse conformers. A completely unhindered bimolecular electron transfer reaction may identify the different electron distributions and in distinct cases can result in different products. It happens during the free electron transfer from phenols (and other chalcogenols) and from benzyltrimethylsilanes to parent ions. This special transfer can be detected when different product ions show different stability, *i.e.* if one of them is stable and the other one dissociates immediately. It is specially true for molecules where good leaving groups exist such as protons (phenol radical cations) or trimethylsilyl cations (here for the silanes **1** and **2**). So the exotic phenomenon is given where a diffusion-controlled reaction reflects intramolecular rotation motions within the donor molecule.

In conclusion, the electron transfer involving σ- or π-type radical cations according to reaction (13) or Scheme 1 should be compared. On the basis of the experimental results and the considerations given above, it can be stated that the saturated parent radical cations ($n\text{-}C_4H_9Cl^{\bullet+}$) react in a manner which is controlled by the molecule dynamics rather than by the mesomeric structure whereas aromatic radical cations ($C_6H_6^{\bullet+}$) seem to follow the latter reaction mode.

Stability of the silane radical cations

In order to interprete the decay of the benzyltrimethylsilane type radical cations two reactions are to be considered. Dinnocenzo *et al.*[3,4] gave convincing arguments for a nucleophile driven bimolecular decay (14).

$$ArCH_2\text{–}SiR_3^{\bullet+} + Nu \rightarrow Ar\text{–}CH^{\bullet}_2 + R_3Si^{+}\cdots Nu \quad (14)$$

Yet, in light of our quantum-chemical calculations, a unimolecular decay should be considered. It accompanies a rotational motion of the C–Si bond from the stable planar radical cation state to the transient perpendicular one. Then the perpendicular transient immediately fragmentates, see reaction sequence (15). Of course, the fragmentation depends strongly on the type and size of the substituents at both neighboring atoms and their electronic effects.

$$ArCH_2\text{–}SiR_3^{\bullet+}{}_{plane} \rightarrow [ArCH_2\text{–}SiR_3^{\bullet+}]_{perp.} \rightarrow Ar\text{–}CH_2^{\bullet} + R_3Si^{+} \quad (15)$$

The data for the rotation times (period of rotation) calculated along the ArC–Si bond both for the ground state and radical cation state are given in Table 2. The rotation times are quite comparable in the case of the ground state molecules, but they differ significantly for the cations $\mathbf{1}^{\bullet+}$ and $\mathbf{2}^{\bullet+}$ (up to a factor of three), which leads to a different decay mechanism.

As can be seen from Fig. 7(b), the decay of the radical cations $\mathbf{1}^{\bullet+}$ is well correlated with the calculated spin densities on the Si atom. Otherwise, the decay of radical cations $\mathbf{2}^{\bullet+}$ is practically independent of the calculated spin densities on the Si atom. This discrepancy could be explained by the essentially slower rotational motion of radical cations $\mathbf{2}^{\bullet+}$ due to the very large substituent R_3.

It is obvious that the decay of $\mathbf{1}^{\bullet+}$ is faster than that of $\mathbf{2}^{\bullet+}$ by at least one order in magnitude. Yet, in the defined experimental conditions another possibility, alternative to the interpretation through rotation frequencies, exists. In the radiolysis of n-butyl chloride a constant amount of the nucleophile Cl^- is generated in the non-polar solvent. So a bimolecular decay reaction of the radical cation derived from the silanes type **1** and $Nu = Cl^-$ could also fit the data. It can be justified by the correlation between spin density at Si and the decay rate of the cations $\mathbf{1}^{\bullet+}$ (*cf.* Table 2), and is further supported by the evidence from other arylmethyl silane systems.[23]

Concluding remarks

It is well known that substantial molecule oscillations, *e.g.*, rotational motions of functional groups at aromatic moieties, are accompanied by the electron fluctuations of the upper occupied orbitals. Consequently, different short-lived conformer states of the molecule come into being and are periodically passed with the rotation frequency. This scenario was set in the time range of hundreds of femtoseconds (chalcogenols[8]) up to a few picoseconds (benzylsilanes, this paper) and has usually no chemical consequences in bimolecular reactions. In this paper the rapid and non-hindered free electron transfer from benzyltrimethylsilane type molecules to parent radical cations of n-butyl chloride is demonstrated. It reflects the intramolecular group rotation and its two characteristic product lines of a bimolecular reaction that, in the end, yield two different conformer silane radical cations. The rotation of the substituents in the benzyltrimethylsilanes was simplified by defining two ground state conformer structures—a perpendicular stable ground state and a planar transient state which have considerably different electron distribution of the HOMO. Through free electron transfer, the aforementioned conformer categories are transformed into the corresponding radical cations which occur without nuclear rearrangement. Of the resulting two types of radical cations, the perpendicular one has dissociative character, whereas the planar one is stable.

The results reported here are in line with the observations in the bimolecular phenol ionization by FET.[8] Therefore the described phenomenon is a more general effect and it is valid for systems with good leaving groups (protons or trimethylsilyl cations) that enable the identification of the different reaction channels, see reactions (4) or (7). In light of the bimolecular chemical reactions philosophy, the described phenomenon represents the molecule dynamics control instead of the usual mesomery determined (encounter complex controlled) product formation.

Experimental section

Materials

n-Butyl chloride has been purified by treating it with molecular sieve (A4, X13) and distillation under nitrogen as described in ref.13. The benzyltrimethylsilanes of types **1** and **2** where synthesized according to literature.[24]

Pulse radiolysis

The liquid samples purged with nitrogen or oxygen were irradiated with high energy electron pulses (1 MeV, 12 ns duration) generated by a pulse transformer electron accelerator ELIT (Institute of Nuclear Physics, Novosibrisk, Russia). The dose delivered per pulse was measured using the absorance of the solvated electron in slightly alkaline aqueous solution, and was usually around 100 Gy. Detection of the transient species was carried out using an optical absorption technique, consisting of a pulsed xenon lamp (XBO 450, Osram), a SpectraPro-500 monochromator (Acton Research Corporation), a R955 photomultiplier (Hamamatsu Photonics) and a 1 GHz

digitizing oscilloscope (TDS 640, Tektronix). Further details of this equipment are given elsewhere.[25]

Quantum-chemical approach

Quantum-chemical calculations were performed using the Gaussian 98, Revision 11 program package[26] based on Density Functional Theory (DFT) Hybrid B3LYP methods[27–29] with a standard 6-31G(d) basis set. The frequency calculations were used to determine the nature of stationary points found by geometry optimisation, and to obtain thermochemistry parameters such as zero-point energy (ZPE) and activation energy E_a (height of rotation barrier).

Acknowledgements

Financial support of this work by the program IKYDA of the German and Greece Academic Exchange Services (DAAD, IKY) is grateful appreciated.

References

1 H. Bock and B. Solouki, *Chem. Rev.*, 1995, **95**, 1161.
2 (*a*) M. G. Steinmetz, *Chem. Rev.*, 1995, **95**, 1527; (*b*) M. Freccero, A. Pratt, A. Albini and C. Long, *J. Am. Chem. Soc.*, 1998, **120**, 284; (*c*) E. Baciocchi, M. Bietti and O. Lanzolung, *Acc. Chem. Res.*, 2000, **33**, 243 and citations herein.
3 K. P. Dockery, J. P. Dinnocenzo, S. Farid, J. L. Goodman, I. R. Gould and W. P. Todd, *J. Am. Chem. Soc.*, 1997, **119**, 1876.
4 H. J. P. de Lijser, D. W. Snelgrove and J. P. Dinnocenzo, *J. Am. Chem. Soc.*, 2001, **123**, 9698.
5 O. Brede, R. Hermann, S. Naumov, G. P. Perdikomatis, A. K. Zarkadis and M. G. Siskos, *Chem. Phys. Lett.*, 2003, **376**, 370.
6 O. Brede, G. R. Mahalaxmi, S. Naumov, W. Naumann and R. Hermann, *J. Phys. Chem. A*, 2001, **105**, 3757.
7 G. R. Mahalaxmi, R. Hermann, S. Naumov and O. Brede, *Phys. Chem. Chem. Phys.*, 2000, **2**, 4947.
8 O. Brede, R. Hermann, W. Naumann and S. Naumov, *J. Phys. Chem. A*, 2002, **106**, 1398.
9 O. Brede, *Res. Chem. Intermed.*, 2001, **27**, 709.
10 *CRC Handbook of Chemistry and Physics*, 73rd edn., CRC Press, Boca Raton, FL, 1992.
11 O. Brede, R. Mehnert and W. Naumann, *Chem. Phys.*, 1987, **115**, 279.
12 (*a*) R. Mehnert, in *Radical Ionic Systems: Properties in Condensed Phases*, eds. A. Lund and M. Shiotano, Kluver, Dordrecht, The Netherlands, 1991, p. 231; (*b*) K. Toriyama, in *Radical Ionic Systems: Properties in Condensed Phases*, eds. A. Lund and M. Shiotano, Kluver, Dordrecht, The Netherlands, 1991, p. 99; (*c*) M. Lindgren and M. Shiotaini, in *Radical Ionic Systems: Properties in Condensed Phases*, eds. A. Lund and M. Shiotano, Kluver, Dordrecht, The Netherlands, 1991, p. 125.
13 R. Mehnert, O. Brede and W. Naumann, *Ber. Bunsen-Ges. Phys. Chem.*, 1982, **86**, 525.
14 A. Kira, Y. Nosaka and M. Imamura, *J. Phys. Chem.*, 1980, **84**, 1882.
15 H. Hiratsuka, Y. Kadokura, H. Chida, M. Tanaka, S. Kobayashi, T. Okutsu, M. Oba and K. Nishiyama, *J. Chem. Soc., Faraday Trans.*, 1996, **92**, 3035.
16 D. C. Neckers, S. Rajadurai, O. Valdes-Aguilera, A. Zakrzewski and S. M. Linden, *Tetrahedron Lett.*, 1988, **29**, 5109.
17 (*a*) D. A. Tasis, M. G. Siskos and A. K. Zarkadis, *Macromol. Chem. Phys.*, 1998, **199**, 1981; (*b*) V. Georgakilas, PhD Thesis, University of Ioannina, Greece, 1998.
18 (*a*) R. F. C. Claridge and H. Fischer, *J. Phys. Chem.*, 1983, **87**, 1960; (*b*) D. Meisel, P. K. Das, G. L. Hug, K. Bhattacharya and R. W. Fessenden, *J. Am. Chem. Soc.*, 1986, **108**, 4706.
19 J. B. Lambert, Y. Zhao, R. W. Emblidge, L. A. Salvador, X. Liu, J.-H. So and E. C. Chelius, *Acc. Chem. Res.*, 1999, **32**, 183.
20 C. Hansch, A. Leo and R. W. Taft, *Chem. Rev.*, 1991, **91**, 165.
21 (*a*) A. K. Zarkadis, PhD Thesis, University of Dortmund, Germany, 1981; (*b*) H. Hillgartner, W. P. Neumann, W. Schulten and A. K. Zarkadis, *J. Organomet. Chem.*, 1980, **201**, 197.
22 O. Brede, S. Naumov and R. Hermann, *Radiat. Phys. Chem.*, 2003, **67**, 225.
23 D. Tasis, M. G. Siskos, A. K. Zarkadis, S. Steenken and G. Pistolis, *J. Org. Chem.*, 2000, **65**, 4274.
24 V. Georgakilas, G. P. Perdikomatis, A. S. Triantafyllou, M. G. Siskos and A. K. Zarkadis, *Tetrahedron*, 2002, 2441.
25 O. Brede, H. Orthner, V. Zubarev and R. Hermann, *J. Phys. Chem.*, 1996, **100**, 7097.
26 M. J. Frisch *et al.*, Gaussian 98, Revision A9, Gaussian Inc., Pittsburgh PA, 1998.
27 A. D. Becke, *J. Chem. Phys.*, 1993, **98**, 5648.
28 A. D. Becke, *J. Chem. Phys.*, 1996, **104**, 1040.
29 Ch. Lee, W. Yang and R. G. Parr, *Phys. Rev. B*, 1987, **37**, 785.